

Inflow-Outflow Solution with Stellar Winds and Conduction near Sgr A*

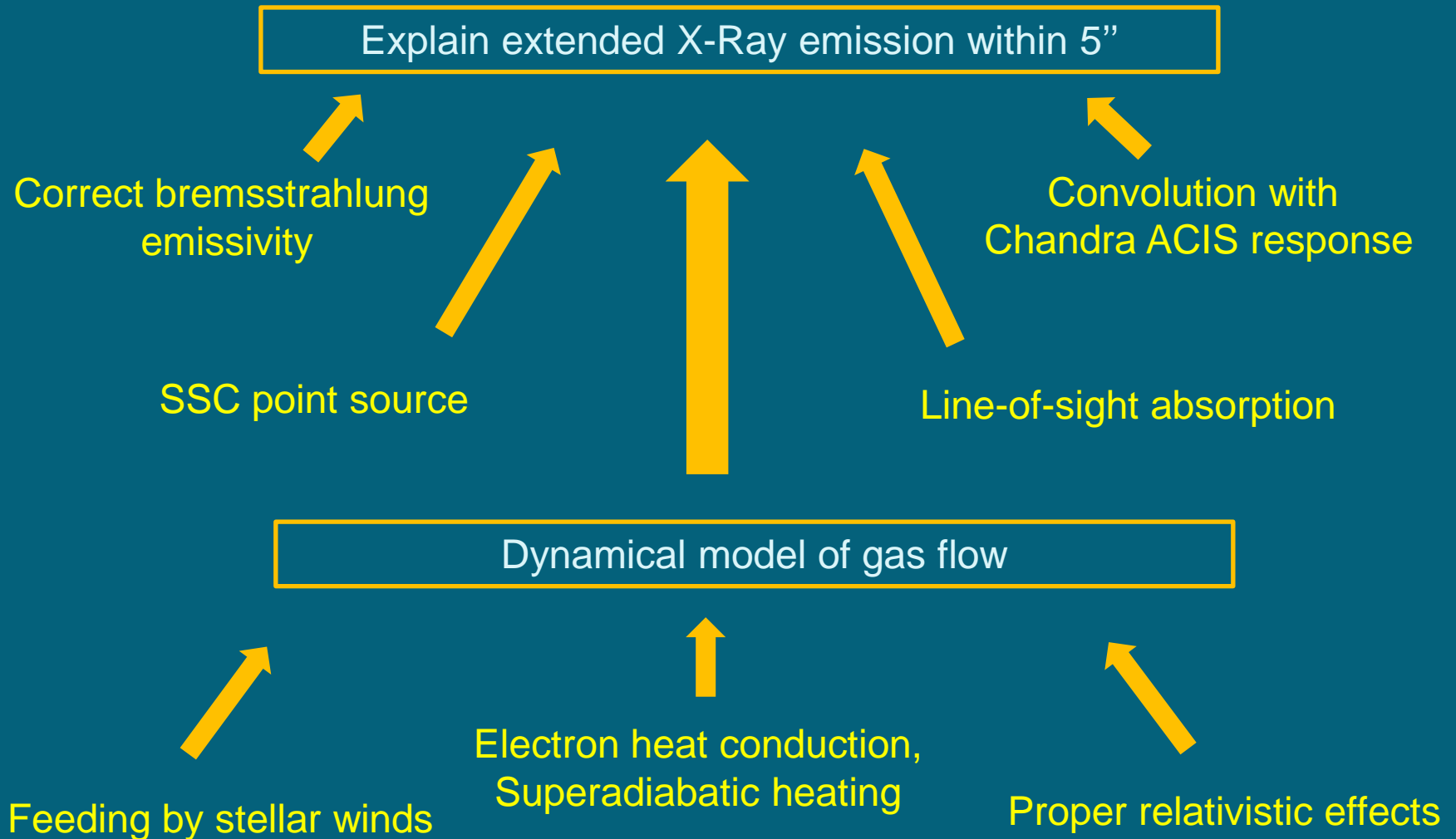
Roman Shcherbakov (Harvard)

Fred Baganoff (MIT)

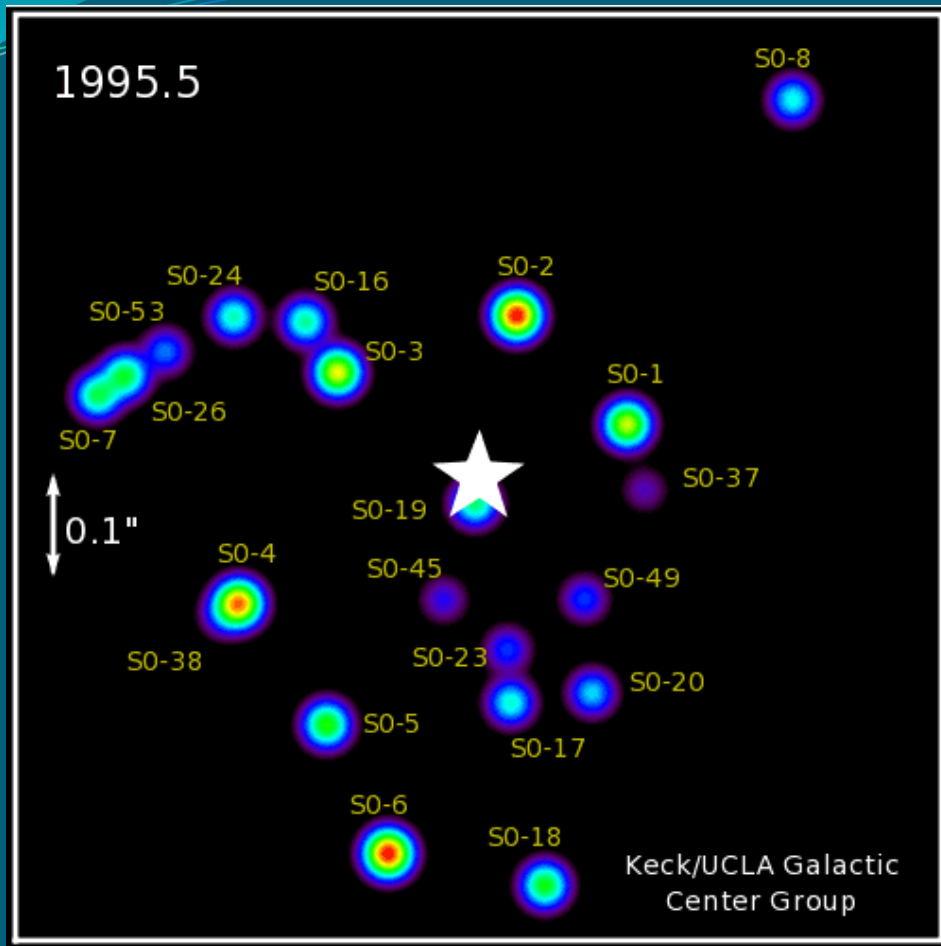
Thanks Ramesh Narayan, Li Ji

Galactic Center Workshop 2009

General idea



Dynamical model: Feeding Mechanism



Stars emit wind at $300 \div 1200 \text{ km/s}$
 ejection rate $\sim 10^{-3} M_{\text{Sun}} / \text{year}$



Winds collide, heat the gas,
 provide seed magnetic field



Most of gas flows out, some accretes

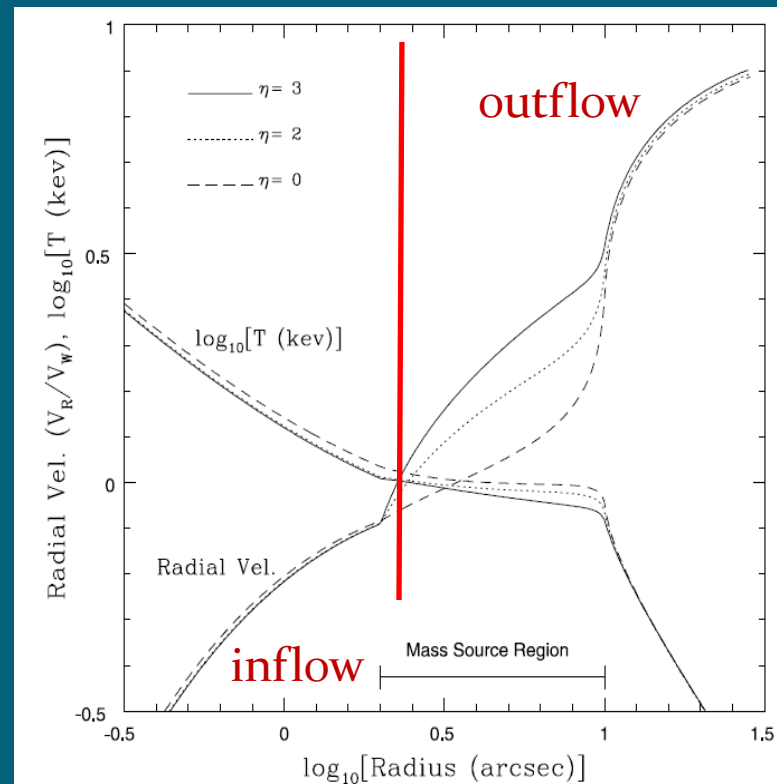


FIG. 1.—Steady state radial velocity and gas temperature as a function of

- Implement realistic feeding, accounting for each star
- Add conduction

Quataert, 2004



1. Simplistic feeding
2. No diffusion/conduction



Dynamical model: Improved Feeding

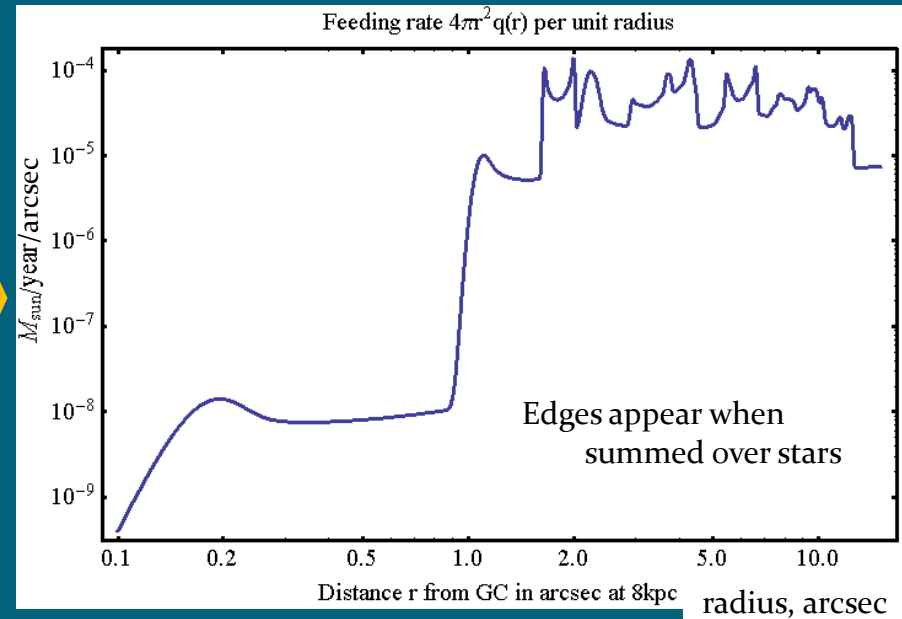
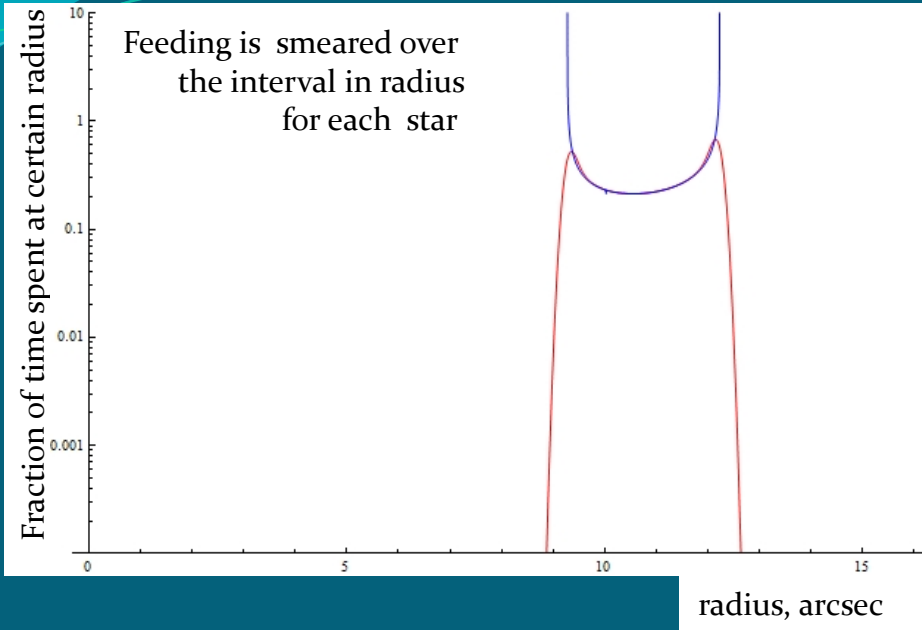
Table of 31 most important wind emitters

N	Ident	$\Delta RA, ''$	$\Delta Decl, ''$	$\Delta z, ''$	$v_{RA}, \text{km/s}$	$v_{Decl}, \text{km/s}$	$v_z, \text{km/s}$	eccentr	$\text{Log}[\dot{M}, M_{\odot}/\text{year}]$	$v_{\text{wind}}, \text{km/s}$
1.	S2, S02	0.04	0.12		9.	1830.	-1060.	0.876	-7.2	1000
19.	IRS16NW	0.029	1.221		238.392	32.9208	-44.	0.898	-4.95	600.
20.	IRS16C	1.121	0.497		-330.722	280.773	125.	0.5	-4.65	650.
23.	IRS16SW	1.051	-0.966	-1.46	257.312	84.0048	320.	0.41	-4.95	600
31.	IRS29N	-1.595	1.423		199.038	-166.874	-190.		-4.95	1000
32.	MPE+1.6-6.8 (16SE1)	1.846	-1.141	-1.52	182.767	112.763	366.	0.26	-4.95	1000
35.	IRS29NE	-0.992	2.073	2.99	-305.369	-10.9736	-100.	0.14	-4.95	1000
39.	IRS16NE	2.868	1.053		117.682	-413.97	-10.	0.	-4.95	1000
40.	IRS16SE2	2.938	-1.183	-1.2	54.4896	130.17	327.	0.206	-4.15	2500.
41.	IRS33E	0.665	-3.126	-3.57	203.579	1.5136	170.	0.63	-4.8	450.
48.	IRS13E4	-3.19	-1.42		-316	76	56.	0.809	-4.3	2200.
51.	IRS13E2	-3.14	-1.74		-303.	68.	40.	0.749	-4.35	750.
56.	IRS34W	-4.05	1.59	1.55	-79.	-166.	-290.	0.217	-4.88	650.
59.	[PMM2001] B9	2.94	3.46		250.	32.	-150.	0.794	-4.9	1000.
60.		-4.36	-1.65		-210.	127.	330.	1.046	-4.95	1000
61.	IRS34NW	-3.73	2.85	3.08	-225.	-112.	-150.	0.	-5.3	750.
65.	IRS9W	2.85	-5.62		167.	135.	140.	0.665	-4.35	1100.
66.	IRS7SW	-3.95	4.93		-5.	-108.	-350.	1.261	-4.7	900.
68.	IRS7W	-2.45	5.99		185.	36.	-305.	0.155	-5.	1000.
70.	IRS7E2 (ESE)	4.41	4.97		203.	-7.	-80.	0.714	-4.8	900.
71.		1.59	6.49		-148.	189.	-300.	0.73	-4.95	1000
72.		6.71	-0.5		65.	100.	86.	0.555	-4.95	1000
74.	AFNW	-7.63	-3.57		-67.	-92.	70.	0.932	-4.5	800.
76.	IRS9SW	4.28	-8.03		108.	8.	180.	0.521	-4.95	1000
78.	[PMM2001] B1	9.46	0.31		-161.	-142.	-230.	0.781	-4.95	1000
79.	AF	-6.54	-6.91		68.	50.	160.	0.991	-4.75	700.
80.	IRS9SE	5.65	-8.17		-2.	-131.	130.	0.766	-4.65	650
81.	AFNWNW	-9.63	-2.58		87.	-9.	30.	0.873	-3.95	1800.
82.	Blum	-8.63	-5.33		-53.	249.	-70.	0.646	-5.3	750
83.	IRS15SW	-1.58	10.02		-55.	-32.	-180.	0.863	-4.8	900.
88.	IRS15NE	1.38	11.68		-8.	103.	-65.	0.877	-4.7	800.

- Orbital data – Paumard et al. (2006)
- Numbers are updated from Lu, Ghez et al. (2009)
- S2 star – Martins, Gillessen (2008)

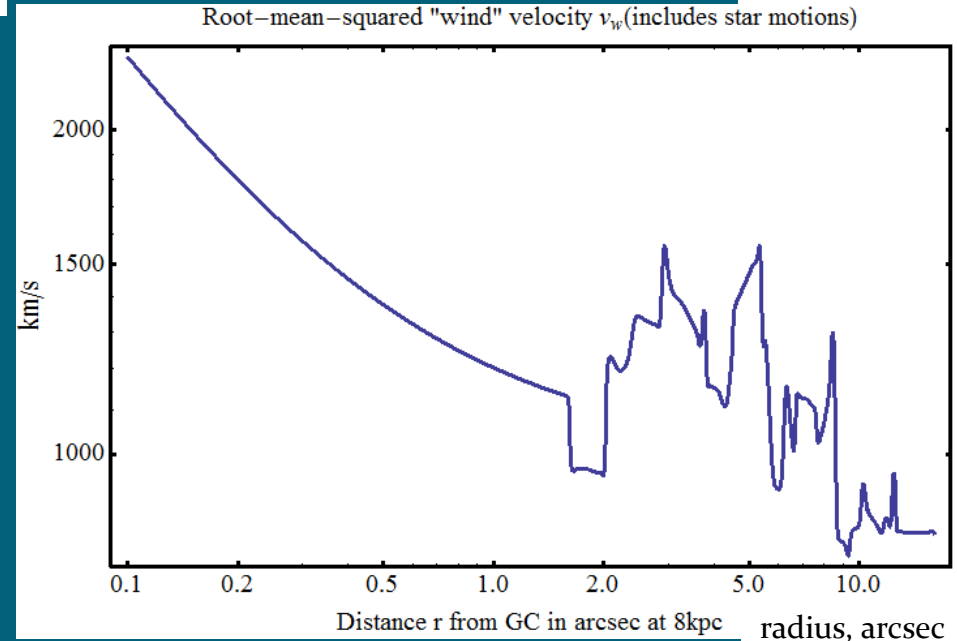
- Δz and Eccentricity – from identification with stellar disks or from minimum eccentricity (if not disk)
- Wind speeds/ejection rate – Martins et al. (2007)
- Guesses on wind speeds/ejection rates from similarity – Cuadra et al. (2007)

Dynamical model: Improved Feeding



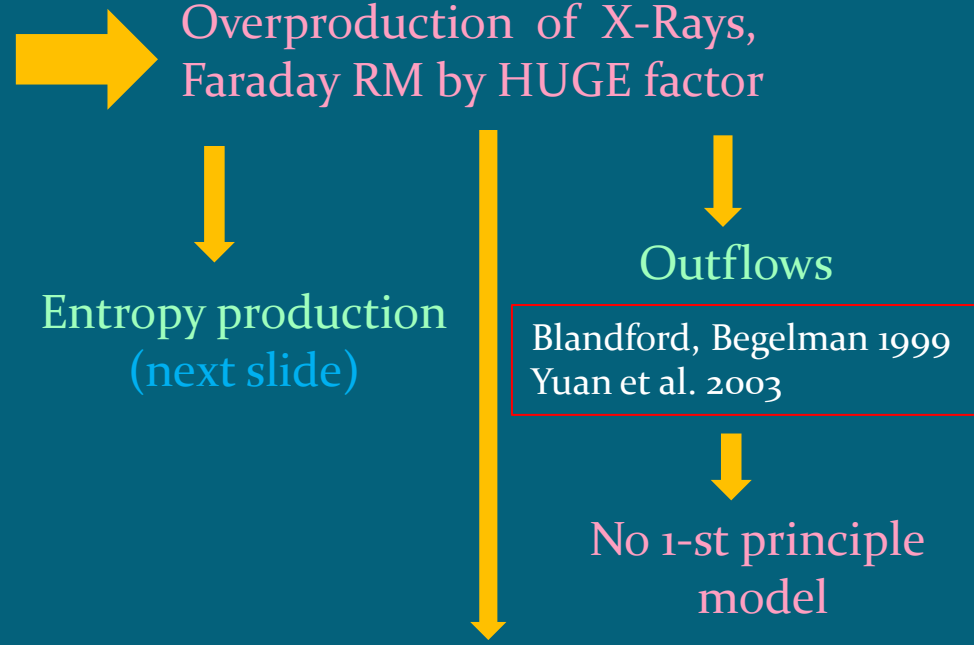
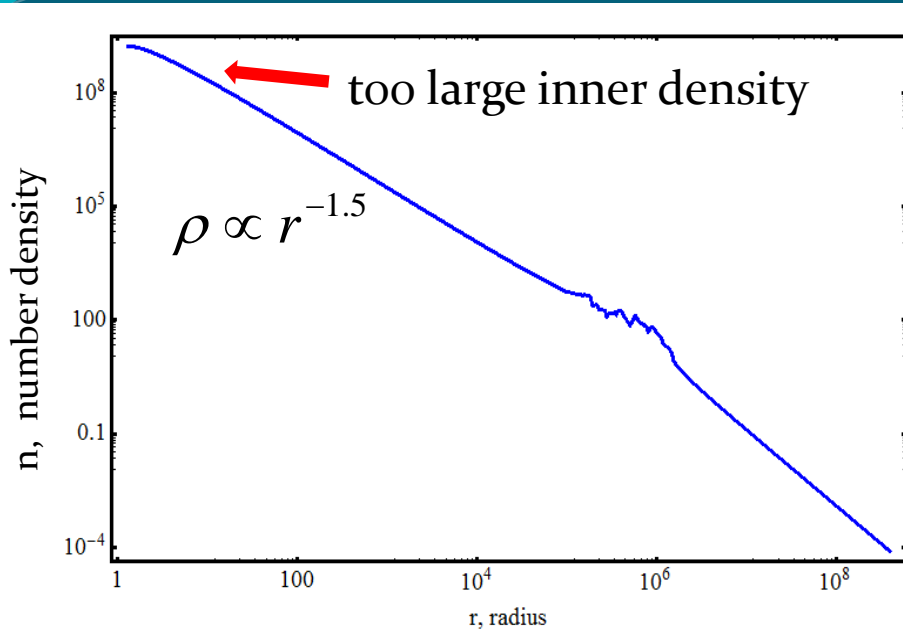
- ✓ Gaussian filter is used to smear out orbits
- ✓ Though orbits are ellipses/hyperboles in 3D, only radial info is retained
- ✓ Slow inflow/outflow + energy equilibration by conduction =>

Radial model is reasonable



Dynamical model: shallow density profile

Adiabatic model without conduction



Why and how electron heat conduction?

- ❖ $v_e \gg c_s \Rightarrow$ electron conduction dominates others
- ❖ saturated collisionless flux or Spitzer value in collisional case
- ❖ damped by a factor 3 to 5 in tangled magnetic field

Narayan, Medvedev 2001

- ❖ heat flux Q_e can be well approximated by

$$Q_e = -\kappa k_B \frac{dT_e}{dr},$$

with conductivity

$$\kappa \sim 0.1 \sqrt{k_B T_e / m_e} \cdot n r$$

Flow is marginally
collisional at 5"

Dynamical model: entropy production

Also called **superadiabatic heating**:
more effective conversion of gravitational energy into thermal

$$-v_r n T_e \frac{ds_e}{dr} = q_e^+$$

$$q_{e,i}^+ = f_{e,i} \frac{GM\dot{M}}{4\pi r^4}$$

Johnson, Quataert 2007

Thin disk



Shakura, Sunyaev, 1971



$$f_i + f_e = 1$$

but we want no cooling

f_i and f_e can be calculated “self-consistently” in turbulent flow

Radial magnetized
turbulent flow



Shcherbakov 2008, ApJ



$$\rho \propto r^{-1.2}$$

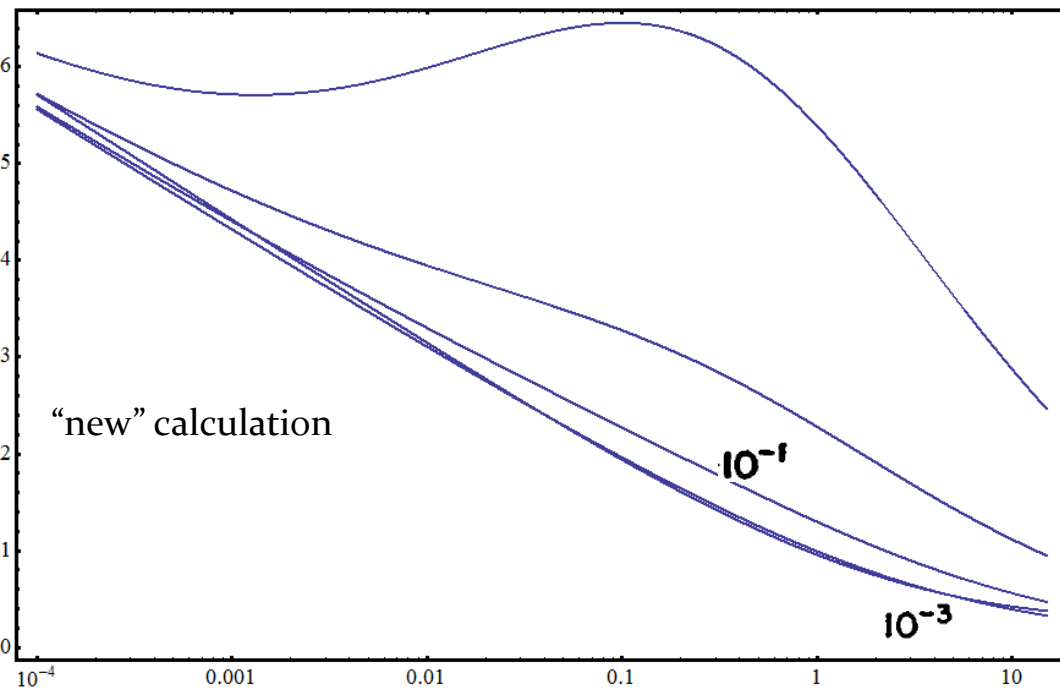
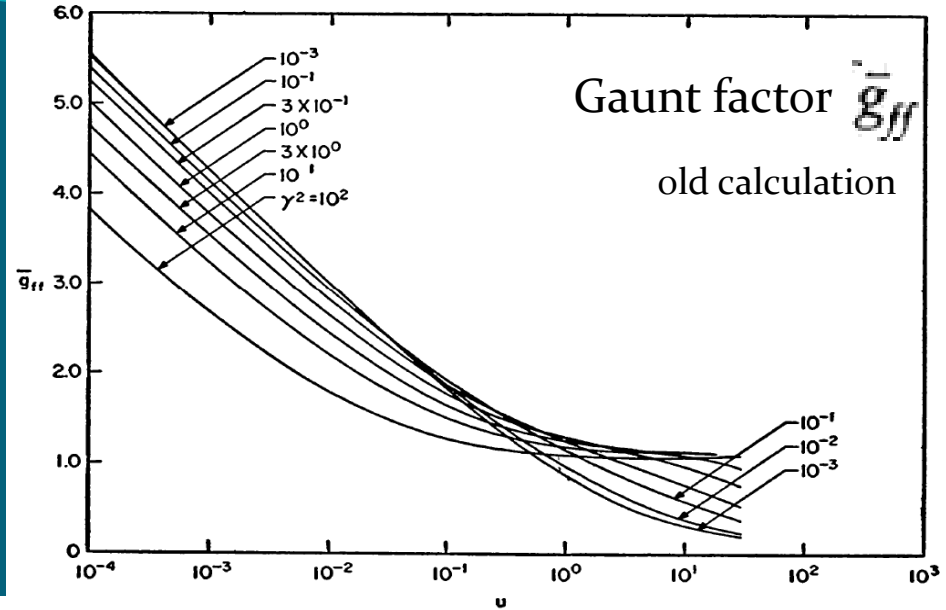
Bremsstrahlung: gaunt factor

$$\frac{dW}{dV dt dv} = \frac{2^5 \pi e^6}{3 m c^3} \left(\frac{2 \pi}{3 k m} \right)^{1/2} T^{-1/2} Z^2 n_e n_i e^{-h\nu/kT} \bar{g}_{ff}$$

$$u = h\nu/kT$$

$$\gamma^2 = Z^2 R y / kT$$

Gould 1980 (+errata)



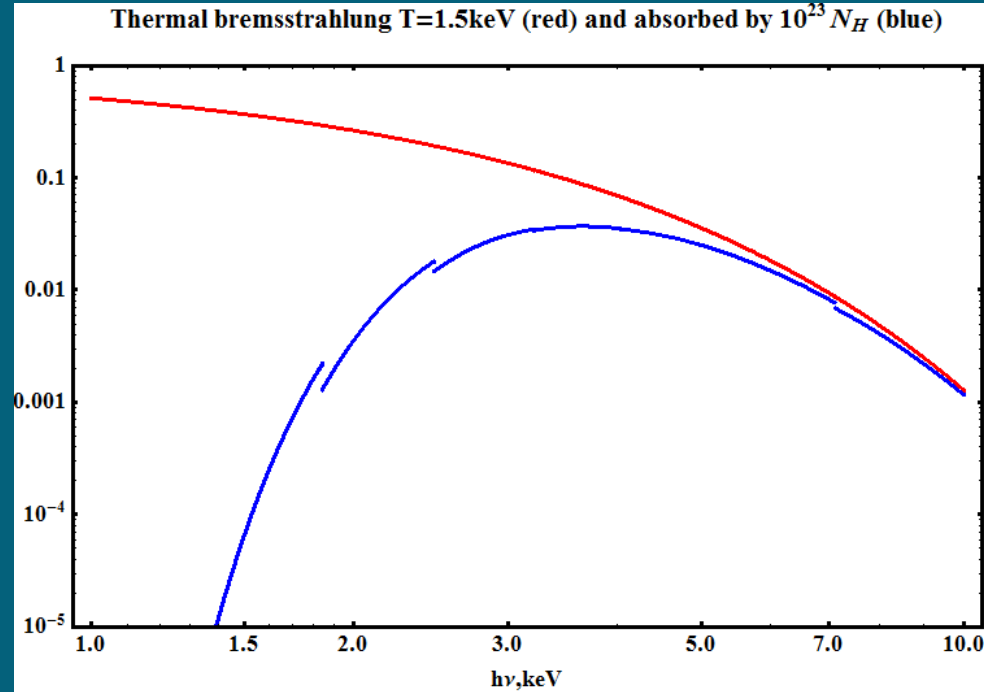
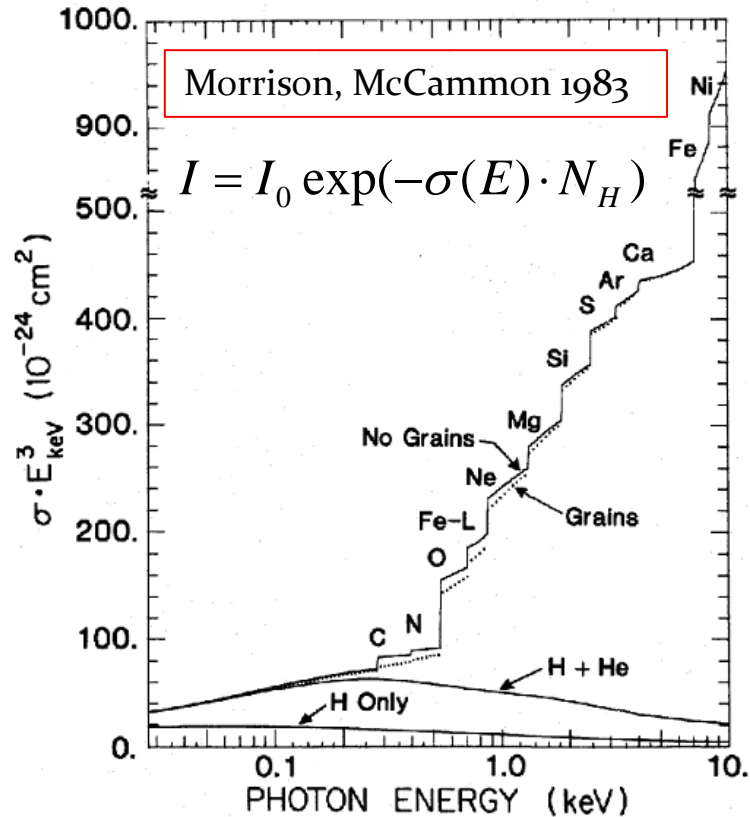
Karzas & Latter 1960

Corrected by
Sommerfeld-Elwert factor
(wave function is not plane wave)

$$f_s(v_f, v_0) = \frac{v_0}{v_f} \frac{1 - \exp(-2\pi\alpha c Z/v_0)}{1 - \exp(-2\pi\alpha c Z/v_f)}$$

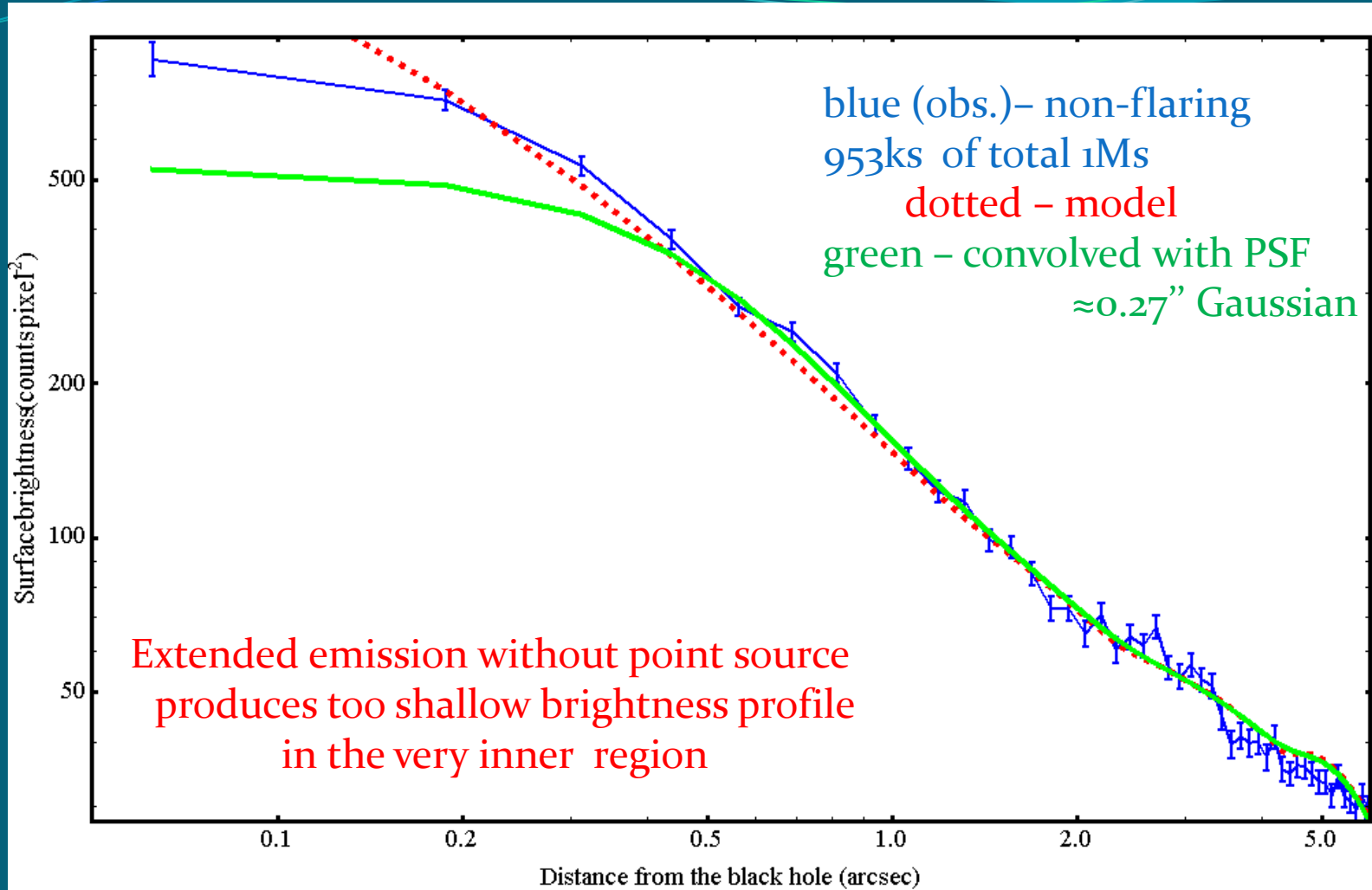
20% larger emissivity
at $T \sim 2\text{keV}$ and $h\nu \sim 4\text{keV}$

Absorption



At $N_H=10^{23}\text{cm}^{-2}$, peak energy reaching the detector is $\geq 4\text{keV}$

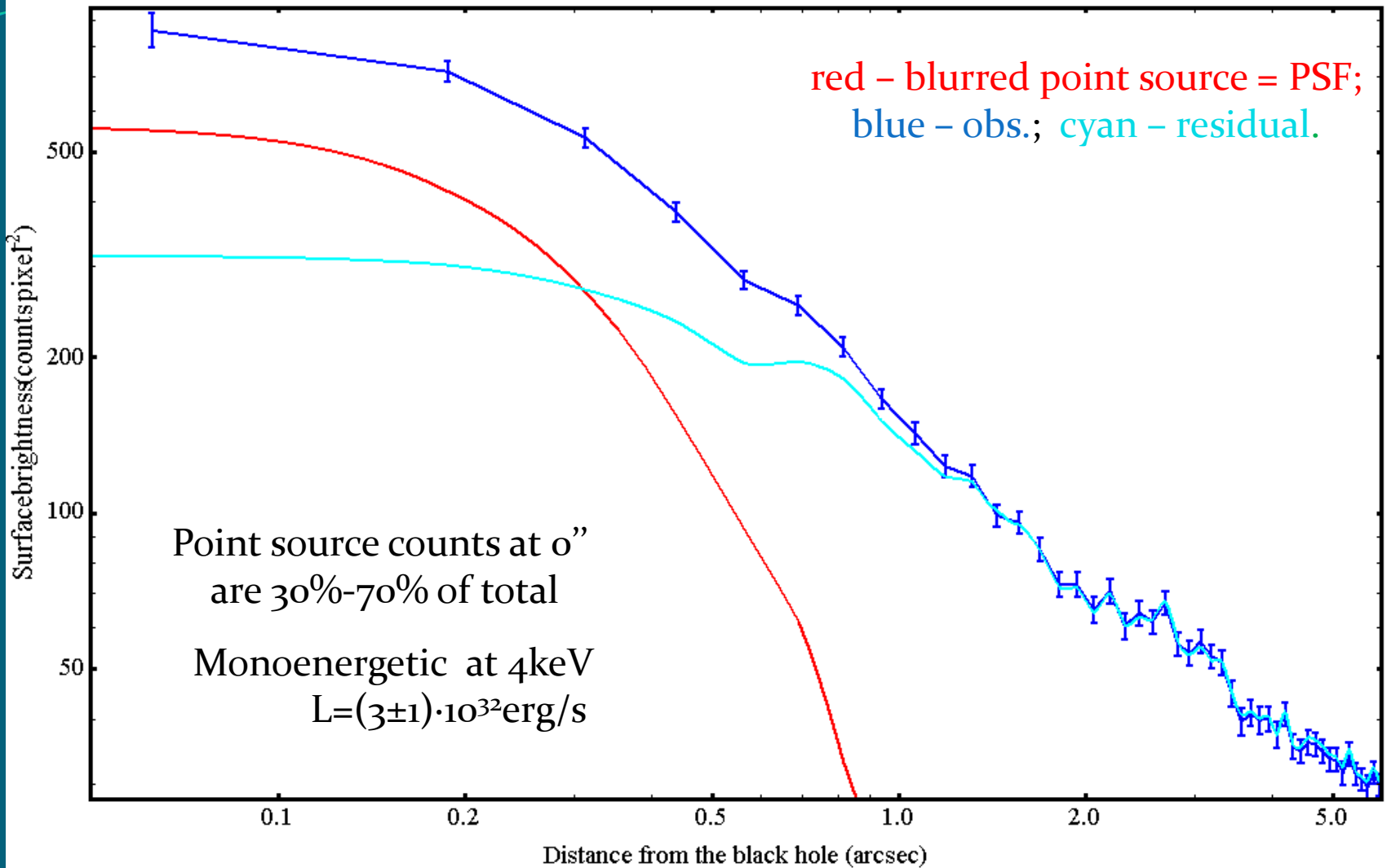
Results: only extended emission



Conduction, $f_i=0.15$, $f_e=0.05$,
relativistic heat capacity of e^-

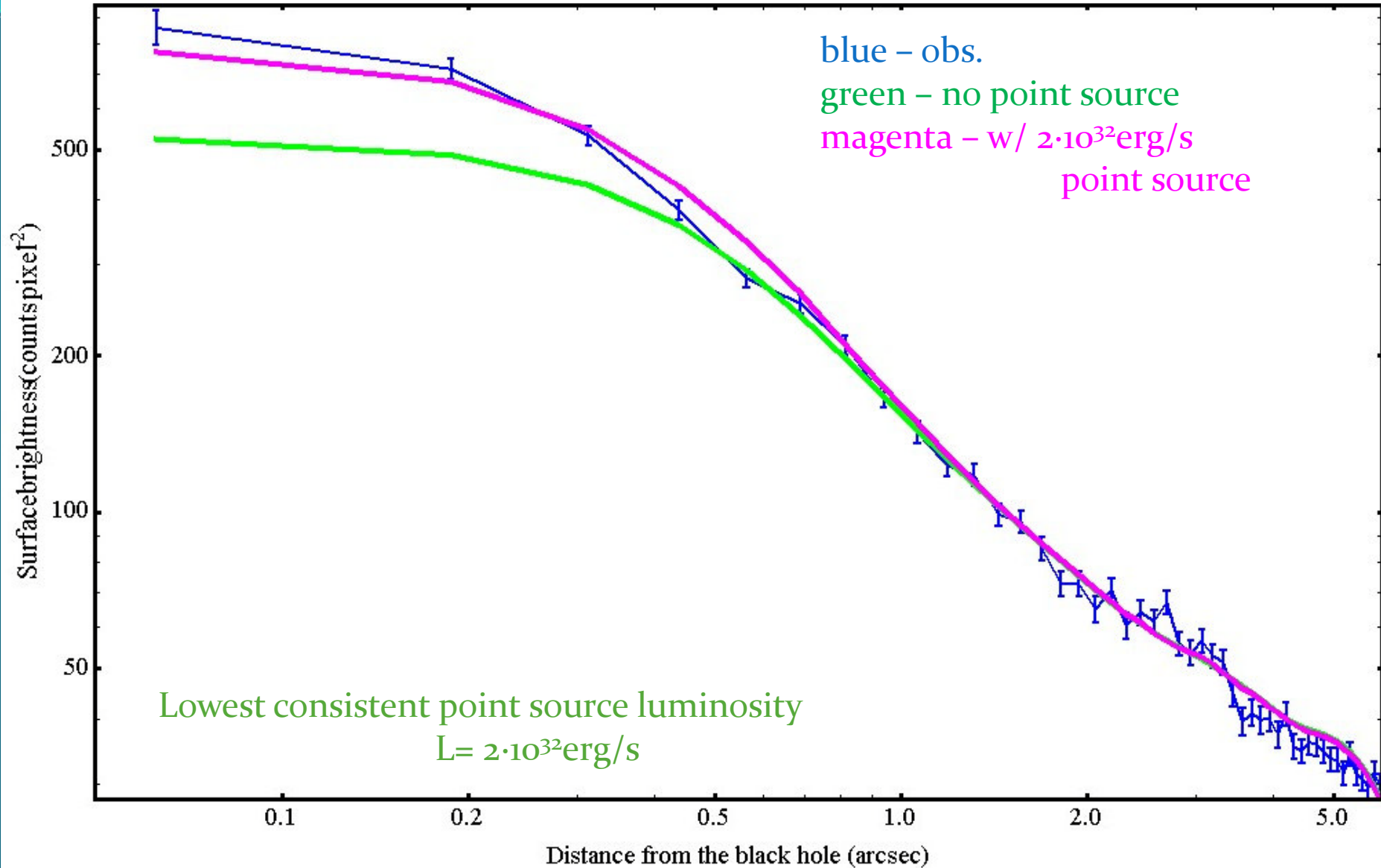
Assumption: emission stops at 7'' (line cooling (Sutherland, Dopita 1993))

Results: point source & residual

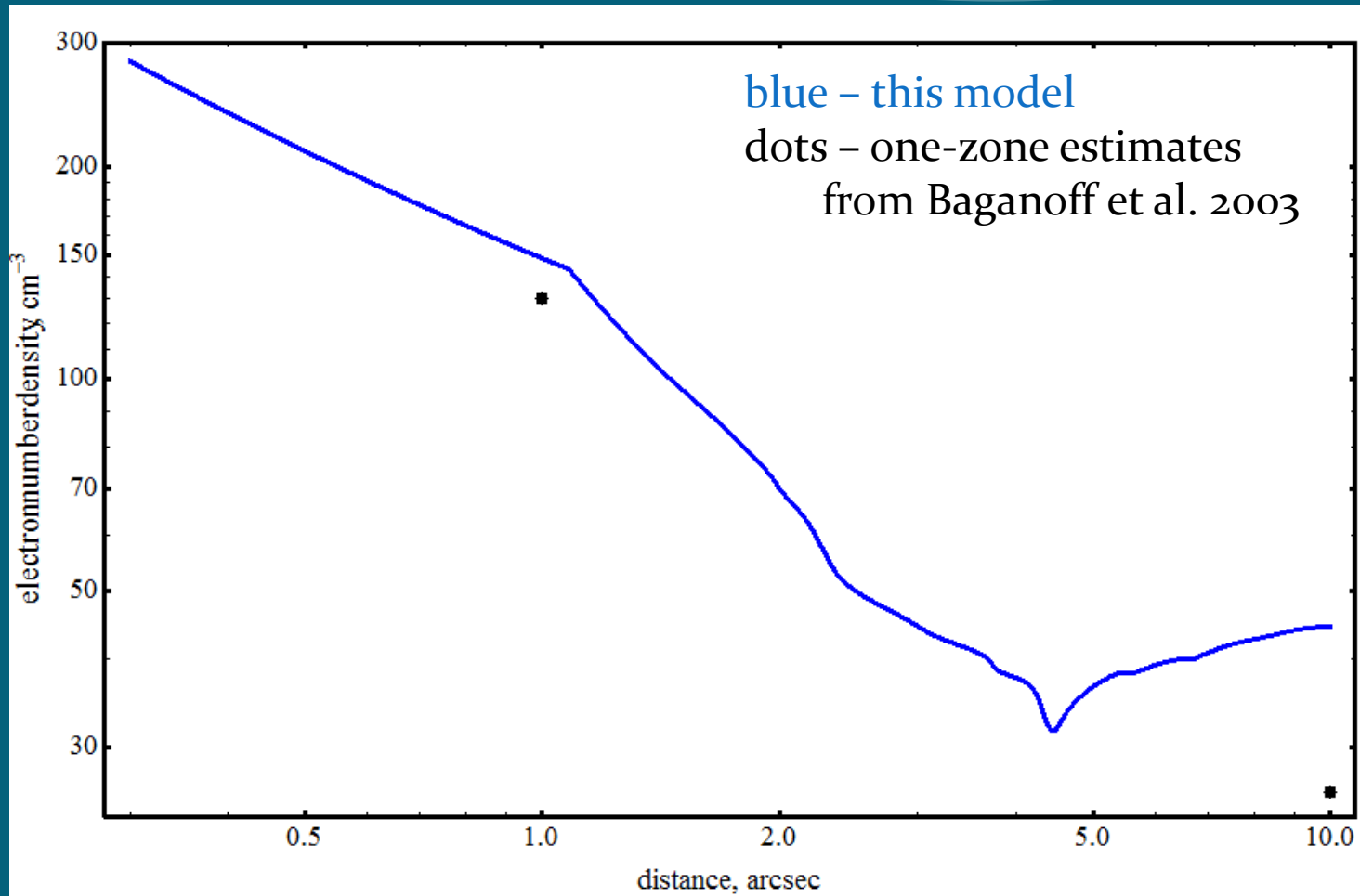


Consistent with Moscibrodzka, et al. 2009
 $\nu L_\nu = 5 \cdot 10^{32} \text{erg/s}$ at 4keV SSC point source

Results: possible fit



Comparison to previous estimates

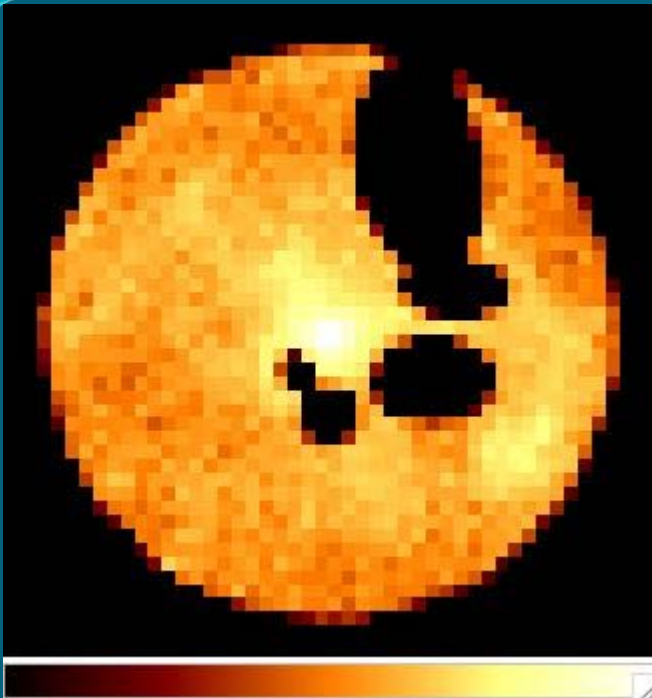


About the same densities in this model
despite bright point sources/extended emission subtracted

Temperature is N_H dependent , around 2.2keV for $N_H=10^{23}\text{cm}^{-2}$

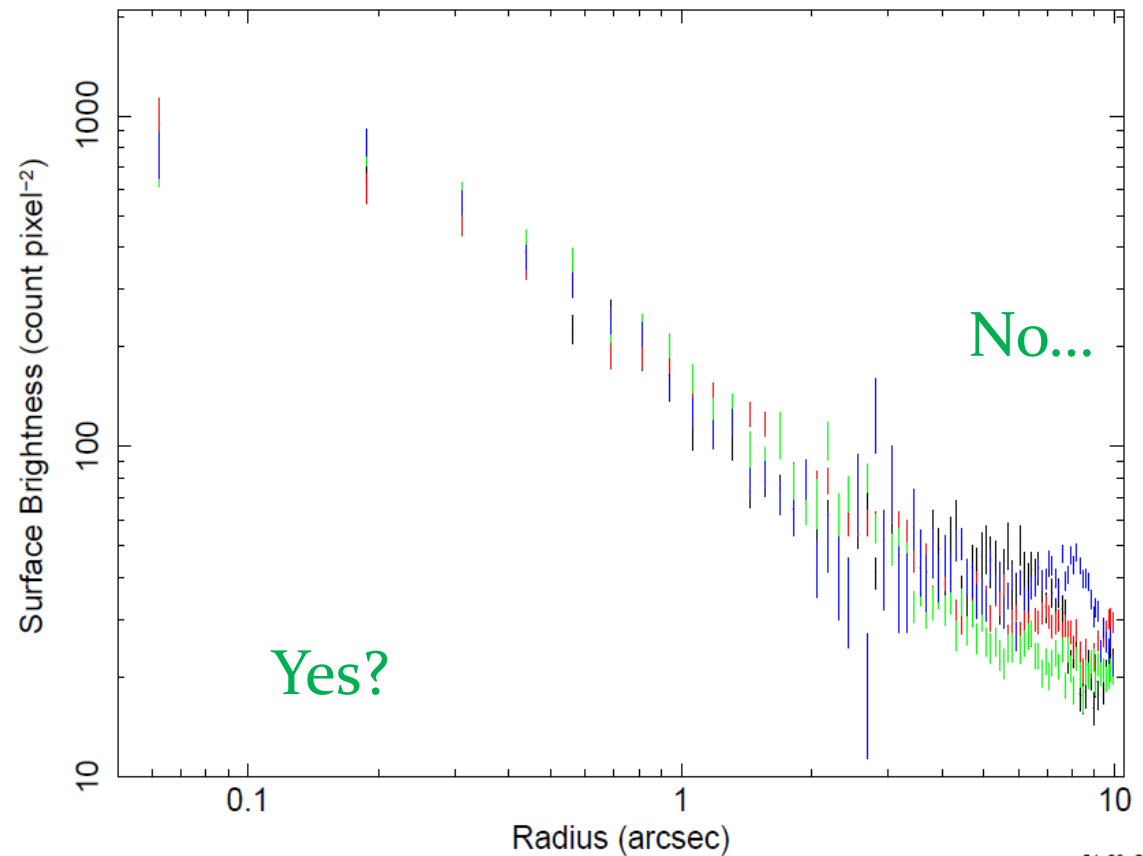
Actually spherically symmetric?

Counts from
4 sectors 90° each



Point sources and
hot streams were subtracted

Plot of file central_pc_rprof_0125as_q1-4.fits



Conclusions

- ✓ Data extracted from extensive Chandra observations (non-flaring)
- ✓ Model constructed with
electron conduction and superadiabatic heating



- ✓ Shallow density profile => fit to extended part of emission
- ✓ Point source of $(3 \pm 1) \cdot 10^{32} \text{erg/s}$ must be present
- ✓ χ^2 search in the parameter space continues

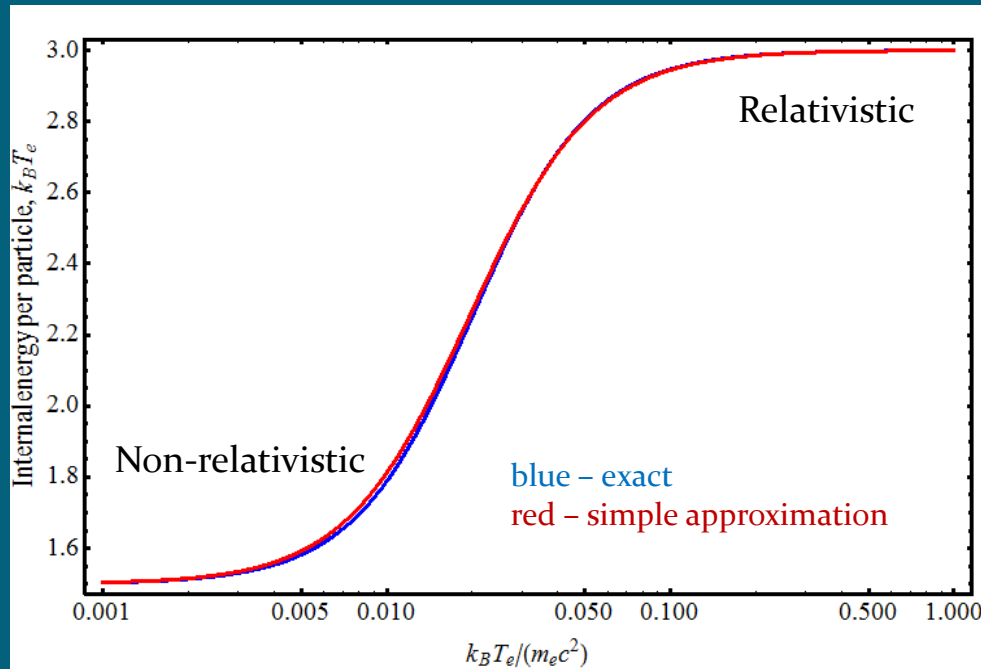
Future work



- ✓ Use spectral data
- ✓ Include angular momentum
- ✓ Fit optically thick sub-mm luminosity (86GHz)

Dynamical model: relativistic effects

Proper heat capacity of relativistic electrons



Non-relativistic heating

$$T_i \sim \rho^{2/3}$$

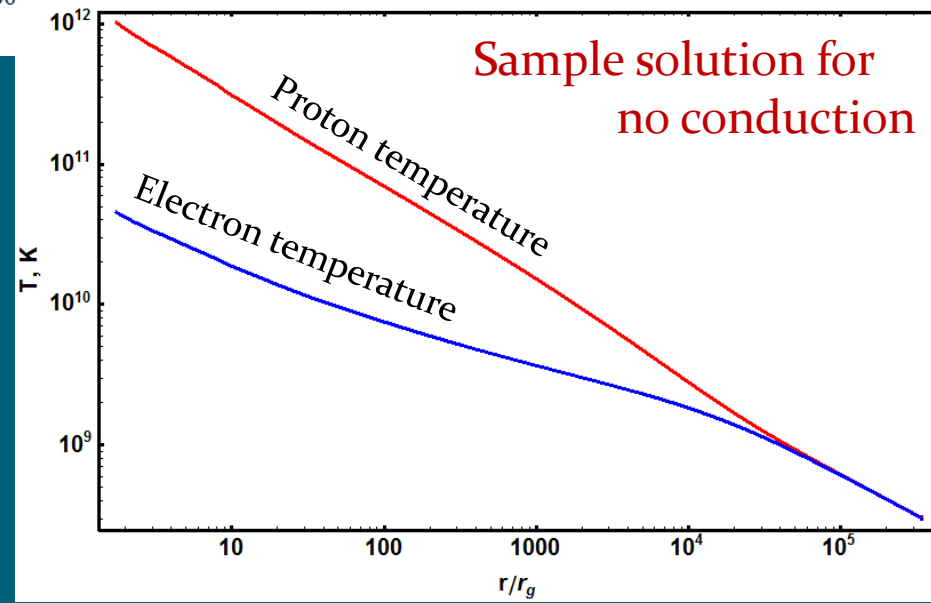
relativistic heating is slower!

$$T_e \sim \rho^{1/3}$$

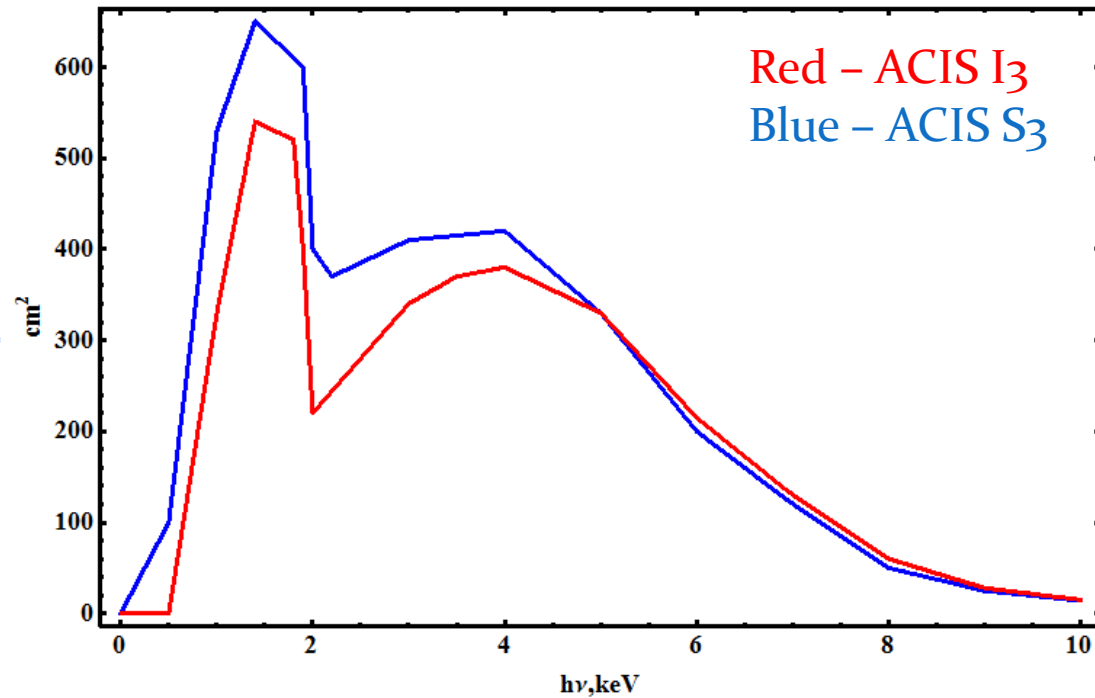
Narayan, McClintock 2008

Temperatures start to deviate at $r < 10^4 r_g$

For adiabatic heating $T_p/T_e = 15$ near BH



Effective area



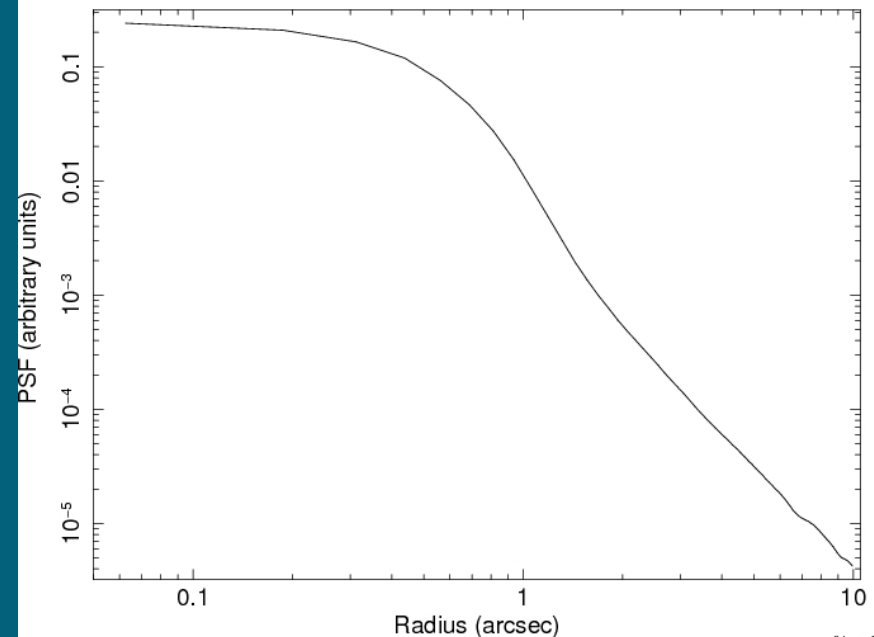
Chandra ACIS response

PSF is well approximated with $\sigma=0.27''$ Gaussian, but has Lorentzian wings



Pixel size $0.492''$, but Dithering of spacecraft allows us to go to subpixel scales!

Plot of file psf_rprof_0125as.fits



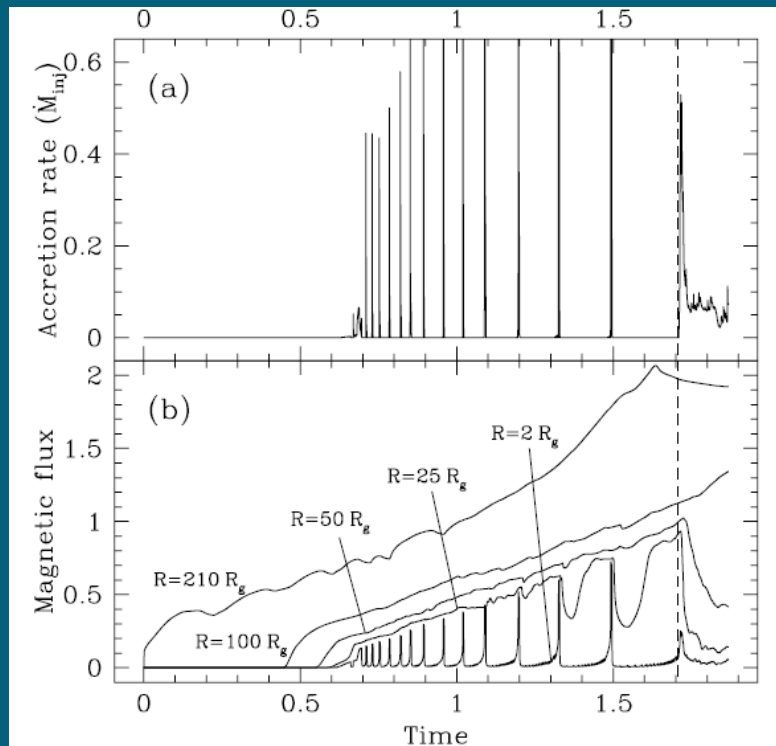
Why 2D GRMHD simulations are bad?

Axisymmetric configurations cannot sustain magnetic field

antydynamo

Ivers, James 1983

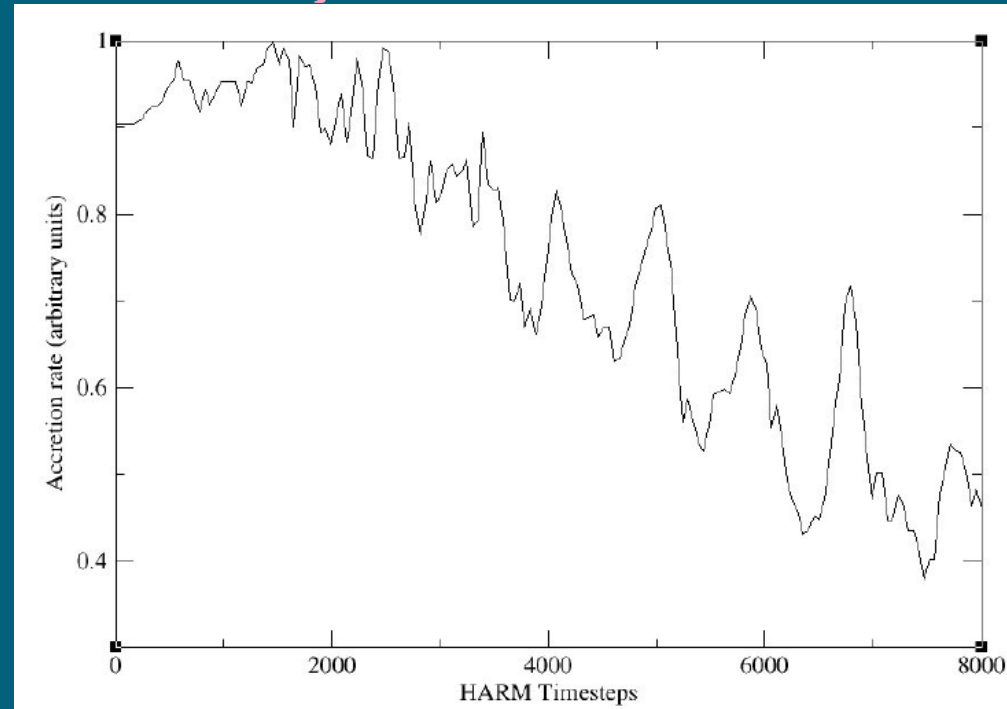
~~Cowling, 1934~~



2D MHD

Igumenshchev 2008

2D flow exhibits cyclic accretion



2D GRMHD

Hilburn, Liang et al. 2009, astro-ph